Atmos. Chem. Phys. Discuss., 8, 13375–13411, 2008
www.atmos-chem-phys-discuss.net/8/13375/2008/

Atmospheric Chemistry and Physics Discussions

Classification of Northern Hemisphere stratospheric ozone and water vapor profiles by meteorological regime

M. B. Follette[1], **R. D. Hudson**[2], **and G. E. Nedoluha**[1]

[1]Naval Research Lab, Remote Sensing Division, Washington, DC, 20375, USA
[2]Department of Atmospheric and Oceanic Science, University of Maryland, College Park, MD 20742, USA

Received: 7 May 2008 – Accepted: 18 May 2008 – Published: 15 July 2008

Correspondence to: M. B. Follette (melanie.follette@nrl.navy.mil)

Published by Copernicus Publications on behalf of the European Geosciences Union.

Abstract

The subtropical and polar upper troposphere fronts serve as the boundaries to divide the Northern Hemisphere into four meteorological regimes. These regimes are defined as (1) the arctic regime – within the polar vortex, (2) the polar regime – between the polar front and the polar vortex, or when the latter is not present, the pole, (3) the mid-latitude regime – between the subtropical and polar fronts, and (4) the tropical regime – between the equator and the subtropical front. Data from the Halogen Occultation Experiment (HALOE) and the Stratospheric Aerosol and Gas Experiment II (SAGE II) were used to show that within each meteorological regime, ozone and water profiles are characterized by unique ozonepause and hygropause heights. In addition, both constituents exhibited distinct profile shapes up to approximately 25 km. This distinction was most pronounced in the winter and spring months, and less in the summer and fall. Both daily measurements and seven-year (1997–2003) monthly climatologies were analyzed.

Daily measurements and seven-year (1997–2003) monthly climatologies showed that, within each meteorological regime, both constituents exhibited distinct profile shapes from the tropopause up to approximately 25 km. This distinction was most pronounced in the winter and spring months, and less in the summer and fall. Despite differences in retrieval techniques and sampling between the SAGE and HALOE instruments, the seven-year monthly climatologies calculated for each regime agreed well for both species below ~25 km. Above this altitude ozone and water vapor profiles were more clearly distinct when binned by latitude rather than by regime.

Given that profiles of ozone and water vapor exhibit unique profiles shapes within each regime in the UTLS, trends in this region will therefore be the result of both changes within each meteorological regime, and changes in the relative contribution of each regime to a given zonal band over time.

ACPD

8, 13375–13411, 2008

1 Introduction

The extratropical upper troposphere/lower stratosphere (UTLS) region is characterized by complex interactions between dynamics, chemistry, microphysics, and radiation. Analyses of these regions are made more difficult by the various definitions of the boundary between the two, the tropopause. The tropopause has been characterized as both a layer (WMO 2003) and a surface (Holton et al., 1995), and there are multiple methods to determine its location.

An important feature of the extratropical tropopause is the break, or split, of the tropopause height across the subtropical and polar upper troposphere fronts. More specifically, as the front is crossed from the equatorward side to the poleward side, there will be a decrease in tropopause height (Bluestein, 1993). This has been widely observed and reported in the literature (Reed, 1955; Defant and Taba, 1957; Danielsen, 1968; Shapiro, 1978, 1980, 1985; Pan et al., 2004). The regions surrounding these fronts will therefore be associated with gradients in tropopause height. Further, the regions away from the fronts will be characterized by relatively little variation in tropopause height (Defant and Taba, 1957; Hudson et al., 2003).

Approximately ninety percent of the total ozone column is located in the stratosphere, and the mid to upper stratosphere is in photochemical equilibrium (Brasseur and Solomon, 1984). Therefore, day-to-day changes in total ozone are dominated by how much ozone is in the mid to lower stratosphere, which is in turn influenced by the height of the tropopause. This relationship between tropopause height and total ozone has been observed in previous studies (Schubert and Munteanu, 1988; Petzoldt et al., 1994; Hoinka et al., 1996; Steinbrecht et al., 1998; Varotsos et al., 2004).

Considering that the subtropical and polar fronts are characterized by changes in tropopause height, and changes in total ozone are correlated with changes in tropopause height, then it follows that the fronts are regions of total ozone gradient (Dobson, 1929; Shalamyanskiy and Romanshkina, 1980; Shapiro et al., 1982; Karol et al., 1987). Hudson et al. (2003, 2006) utilize these gradients in the total ozone field to

ACPD
8, 13375–13411, 2008

locate the positions of the subtropical and polar fronts.

Hudson et al. (2003) found that these fronts, along with the polar vortex, divided the Northern Hemisphere total ozone field into meteorological regimes, which they defined as (1) the arctic regime – within the polar vortex, (2) the polar regime – between the polar front and the polar vortex, or when the latter is not present, the pole, (3) the midlatitude regime – between the subtropical and polar fronts, and (4) the tropical regime – between the equator and the subtropical front. They used data from the TOMS instruments, rawinsondes, and ozonesondes to show that, with the exception of the arctic, the regimes, while encompassing a large range of latitudes and longitudes, were found to have relatively constant values of total ozone, tropopause height, and ozonepause height (Hudson et al., 2003, 2006).

This paper will utilize the concept of meteorological regimes as defined by Hudson et al. (2003, 2006) to examine ozone and water vapor profiles from the Halogen Occultation Experiment (HALOE) and the Stratospheric Aerosol and Gas Experiment II (SAGE II) outside the frontal regions. The motivation is to determine how well, and over what altitude ranges and seasons, stratospheric ozone and water vapor profiles can be usefully differentiated by meteorological regime. Understanding the extent to which variations in these constituents are determined by meteorological regime is an important component to understanding any trends in water vapor and ozone in the UTLS. A brief description of the data used follows in Sect. 2. Section 3 provides an explanation of the method used to classify the profiles into meteorological regimes. Sects. 4 and 5 will show the results of the ozone and water vapor analyses, respectively. The summary and discussion will follow in Sect. 6.

ACPD

8, 13375–13411, 2008

2 Data

2.1 TOMS

The Total Ozone Mapping Spectrometer (TOMS) instruments measure backscattered solar ultraviolet (UV) and provide daily high-resolution global maps of total ozone. This paper uses the level-3 version 8 Earth Probe (EP) TOMS data on a 1° latitude by 1.25° longitude grid. EP TOMS made measurements from July 1996–December 2005. According to the TOMS website (http://jwocky.gsfc.nasa.gov/news/news.html#aug15), instrument degradation reduced the accuracy of the ozone retrieval after mid-2000. The TOMS data is corrected using NOAA-16 SBUV/2 measurements and should therefore not be used for trend analyses. Since this paper relies primarily on the spatial variability of the TOMS data these results are not significantly affected by uncertainties in the trend. Error analyses suggest that the total ozone has an rms error of about 2% (Wellemeyer et al., 2004, and references therein). These errors are at a maximum at high solar zenith angles and in the presence of heavy aerosol loading, and are not expected to interfere with this analysis, as we will limit ourselves here to the study of profiles for which the maximum latitude is 60° N.

2.2 HALOE

Data from the HALOE instrument has been widely used to study the chemistry of the stratosphere because of its global coverage, its coincident measurements of several key chemical species, and its relatively long time period (1991–2005). It was on board the Upper Air Research Satellite (UARS) and was launched on 15 September 1991 into a 585 km, 57° inclination orbit. The HALOE instrument started taking observations on 11 October 1991 after a brief period of outgassing, and ceased operation on 21 November 2005. The experiment was devised to observe not only ozone but also several other species that have direct effects on ozone levels, namely hydrochloric acid (HCl), hydrogen fluoride (HF), methane (CH_4), water vapor (H_2O), nitrogen dioxide

ACPD
8, 13375–13411, 2008

(NO_2), and nitrous oxide (NO), in order to gain a better understanding of the chemistry and dynamics of middle-atmosphere processes (Russell et al., 1993). Vertical profiles of these constituents were measured along with aerosol extinction and temperature versus pressure.

HALOE was a limb-scanning solar occultation instrument. The satellite orbit precessed, covering from ~80° N–80° S over a year. The maximum sampling for each day was 15 sunrise and 15 sunset measurements, most of the time in opposite hemispheres. During an occultation event, all of the chemical species listed above were measured. Depending on the channel, the altitude range sampled was from 15 to ~60–130 km, with a vertical resolution of about 2.3 km, and a horizontal resolution of ~200 km (SPARC, 2000).

Validations have been done on the various versions of the HALOE ozone data (Brühl et al., 1996; Bhatt et al., 1999). The HALOE version 19 level 3 data has been used here. This data has also been screened for cirrus cloud contamination using the method described in Hervig and McHugh (1999). The sunrise and sunset data have been combined and show differences less than 5% above 100 mb (Brühl et al., 1996). In the lower stratosphere, the major systematic and random uncertainties in the ozone data are between 9 and 25% (Brühl et al., 1996; Grooß and Russell, 2005). Bhatt et al. (1999) found agreement with coincident ozonesonde measurements better than 10% down to 200 mb, and better than 20% down to 300 mb in the extratropics. In the tropics and subtropics, the agreement was better than 10% down to 100 mb.

The water vapor channel measures solar infrared radiation at 6.6 μm. At this wavelength, other species are unlikely to contaminate the signal, although absorption by aerosols can have an effect. After the eruption of Mt. Pinatubo, this channel was opaque below 35 km near the equator (Harries et al., 1996). For water vapor profiles, the combined systematic and random errors in the lower stratosphere are 14–24% (Grooß and Russell 2006). Kley et al. (2000) performed an extensive validation, and found that HALOE v19 water vapor profiles agreed with correlative measurements within ~10% throughout most of the stratosphere. Differences increase somewhat in

ACPD
8, 13375–13411, 2008

the upper stratosphere and near the tropopause.

2.3 SAGE II

The SAGE II instrument was launched on board the Earth Radiation Budget Satellite (ERBS), and was operational from 5 October 1984 to 26 August 2005. SAGE II (hereafter referred to as SAGE) was a seven-channel sun photometer that used solar occultation to infer vertical profiles of ozone, water vapor, NO_2, and aerosol extinction at several wavelengths from 0.385–1.02 μm. Similar to HALOE, SAGE was launched into a 610 km, 57° inclination precessing orbit that covered from ~70° S to ~70° N, and made a maximum of 15 sunrise and 15 sunset measurements per day (Cunnold et al., 1989). The vertical resolution was 1 km (Chu et al., 1989), and the horizontal extent along the line of sight was 200 km by 2.5 km for a 1-km retrieved layer (WMO 1998).

For SAGE ozone profiles, the dominant source of error is the measurement error, but the total random error for a 1-km vertical resolution is less than 7% between 2 km above the tropopause and 43 km (Cunnold et al., 1989). Better than 10% agreement between SAGE version 6.1 ozone measurements and coincident ozonesonde measurements was found down to the tropopause (Wang et al., 2002). In addition, Randall et al. (2003) found that HALOE v19 and SAGE v 6.1 ozone profiles agreed within 5%, and Morris et al. (2002) reported virtually no drift in the HALOE v19 ozone observations with respect to SAGE II v 6.0. Version 6.2 of the SAGE data is used in this paper. This data differs little from the previous version[1], v 6.1.

Version 6.2 SAGE water vapor profiles, though still affected by the presence of aerosols, have reduced sensitivity with respect to previous versions. The retrievals were modified to remove the dry bias with respect to the HALOE water vapor profiles (Thomason et al., 2004). When SAGE water vapor profiles were compared with

[1]"For the most part, the ozone density profiles have changed on the order of 0.5% from version 6.1. The changes may be larger above 50 km and are due primarily to the correction of an altitude registration problem in our NCEP gridding algorithm." Taken from http://www-sage2.larc.nasa.gov/data/v6/data/

ACPD
8, 13375–13411, 2008

both ground-based and satellite correlative measurements, good agreement of within 10% was seen from 15–40 km. Comparison between data sets in the region of the hygropause is more difficult, given the increase in atmospheric variability and differences in the techniques and ability of each platform in resolving this region. However, SAGE comparisons with balloon-borne frost-point hygrometers and MkIV interferometers showed agreement around the hygropause to within 10% (Taha et al., 2004).

3 Method

As explained in the introduction, Hudson et al. (2003, 2006) utilize gradients in the total ozone field to locate the positions of the subtropical and polar fronts. A detailed description of the procedure used can be found in Hudson et al. (2003), and a revision to this method is described in Hudson et al. (2006). While the subtropical and polar fronts are calculated based on total ozone gradients, the polar vortex boundary is determined from the position of the sharpest gradient in PV on the 550 K potential temperature surface. The PV data were obtained from the National Centers for Environmental Prediction/National Center for Atmospheric Research (NCEP/NCAR) reanalysis data set (Kalnay et al., 1996, Kistler et al., 2001).

Every profile measured by HALOE and SAGE has an associated latitude, longitude, time, and date. These were used to locate the corresponding location on the TOMS image for that day in order to classify the profile into a particular meteorological regime. Both retrieval algorithms assume a homogenous atmosphere for their calculations (Chu et al., 1993). However, as explained above, the region around the front represents a discontinuity in tropopause height (i.e. an inhomogeneous atmosphere) that will not be accounted for in the retrieval. For this reason, profiles that fell near a boundary region were not included in the analysis. In the present work we have expanded the boundary regions, as defined using the TOMS data, from the one pixel range to an average of three pixels. This one pixel expansion of the boundary region in both latitude and longitude generally insures that the regimes are clearly differentiated, but we do

ACPD
8, 13375–13411, 2008

note that, especially from about June to October, the ozone gradient weakens and the transition region from one regime to another becomes broader. Misclassification could also occur because of different measurement times. EP TOMS measurements are made at approximately 11 a.m., whereas both SAGE and HALOE measurement are made at local sunrise or sunset. For example, in the case of sunrise measurements, the total ozone field that is measured by TOMS could have shifted with respect to the total ozone field at sunrise that day. This source of error will depend on the time of year, as weather patterns are more persistent in summer and fall.

Ozone profiles from SAGE and HALOE, from 25°–60° N, were classified into meteorological regimes for every day that there were both profile measurements and EP TOMS data available between January 1997 and December 2003. This time period was chosen for several reasons. As stated above, HALOE began taking measurements in 1991, and SAGE began in 1984. However, due to the eruption of Mount Pinatubo in June 1991, measurements below 25 km for HALOE (WMO 1998), and below 20 km for SAGE (Wang et al., 2002) until the end of 1993 are contaminated by aerosols. In addition, Nimbus-7 TOMS data ceased in May 1993, and the Meteor-3 data has many months missing. Thus, January 1997, near the beginning of the EP TOMS data period, was chosen as the starting point.

Ozonepause and hygropause heights were also determined for every profile. The sharp increase in ozone from the troposphere to the stratosphere can be used to find the position of the "chemical tropopause" or "ozonepause". Unlike other definitions, there is no standard definition for the ozonepause. Bethan et al. (1996) defined a tropopause based on the lowest altitude where the ozone profile met the following three criteria,

- The vertical gradient in ozone mixing ratio exceeds 60 ppbv km^{-1} over a depth of approximately 200 m
- The ozone mixing ratio is greater than 80 ppbv
- The ozone mixing ratio immediately above the tropopause is greater than 110 ppbv

ACPD
8, 13375–13411, 2008

We have adopted the Bethan et al. (1996) definition for this paper. Because the SAGE and HALOE data become noisy near and below the ozonepause (Grooß and Russell 2005; Randel et al., 2007), an additional criterion requiring the vertical gradient 2 km above the ozonepause to be positive was added. This will also filter out most stratospheric intrusions into the troposphere. However, the "higher" tropopause will be the one most relevant to this work, as it is the one that will have the greatest effect on the column. The hygropause was defined as the altitude of the water vapor minimum (Kley et al., 1979).

4 Ozone profile classification

4.1 One day

Hudson et al. (2003) showed that when Northern Hemisphere rawinsonde and ozonesonde data were divided into meteorological regimes, similar profile shapes were seen within each regime. Figure 1 shows the EP TOMS total ozone field for 18 February 1998 in addition to the subtropical, polar, and polar vortex boundaries, shown as blue, red, and black lines, respectively. Each symbol on this figure represents a sunset HALOE event for this day, and has been assigned a number from 01 through 15. The HALOE measurements are approximately 24 degrees of longitude apart. The color and choice of symbol corresponds to its classification: blue triangles – polar; purple diamonds – midlatitude; red squares – tropical; black X's – boundary. All of the profiles for this day are plotted in Fig. 2, although only those that fell within a regime are in color and listed on the figure. HALOE profiles are present in all three regimes on this day, in addition to several boundary-classified profiles that have been eliminated. In order to examine these profiles closely, Fig. 3a–c show the individual profiles that have been classified as polar, midlatitude, and tropical, respectively. The polar profiles for this day are seen in Fig. 3a. These profiles have very similar profile shapes and ozonepause heights, 7–8.5 km, despite being very far apart in longitude. The two tropical profiles in

ACPD
8, 13375–13411, 2008

Fig. 3c also have similar shapes and show ozonepause heights at around 16–17 km. Figure 3b shows five midlatitude ozone profiles. These too also show similar profile shapes, however their ozonepause heights range from 10 to approximately 15 km, a much larger range than in the polar or tropical regimes.

This day is a good example of the advantage of classifying profiles by meteorological regime. All of the HALOE measurements seen in Fig. 3 are located within ~4° latitude of each other, as all of them fall between approximately 41° and 44° N, yet they show distinctly different profile shapes in the lower to mid stratosphere. Thus, if a zonal average over this very small latitude band was calculated at 15 km, it would contain both upper tropospheric and lower stratospheric air. By classifying these profiles by meteorological regime, the lower stratosphere can be isolated. This is essential for the examination of ozone trends in the UTLS.

4.2 Climatology

Data from both HALOE and SAGE are used to calculate monthly climatologies for each regime over the time period 1997–2004 between 25° and 60° N. Figure 4a–d show the March, June, September and December ozone profile climatologies, respectively, calculated using data from the HALOE instrument for the subtropical (red), midlatitude (green), and polar (blue) regimes. The standard deviation (1σ) is shown as dashed lines on either side of the mean profile, and the number of points used is shown on the right, in each plot. Both the number of points and the standard deviations have the same color scheme as the mean profiles. Due to the nature of HALOE's orbit, some months had limited sampling in certain regimes. If the number of profiles available for a regime was below 20, the mean was not included.

In the lower stratosphere, the climatological profiles show distinct ozonepause heights within each regime for every month, except for the tropical and midlatitude regimes in September. In late summer and early fall, the latitudinal gradient in the total ozone field is at a minimum. Therefore, the difference in mean total ozone from one regime to the next is at a minimum (Hudson et al., 2006), as is the difference

ACPD
8, 13375–13411, 2008

in tropopause height. In Fig. 4a, b, and d, however, the 1σ distributions barely overlap in the UTLS, if at all. Above approximately 25 km, however, profiles are in most cases not well differentiated by regime. In Fig. 4a for example, the midlatitude and polar climatologies are almost identical above this altitude. This will be discussed further below. The monthly mean ozonepause heights for the tropical (red), midlatitude (green) and polar (blue) regimes are shown in Fig. 5 and are consistent with the results shown in Figs. 2–4; the highest ozonepause heights are seen in the tropical regime, and the lowest in the polar. Similar to Fig. 4, the one-sigma standard deviation of the means are shown as dashed lines on either side of the means. The overlapping distributions seen in Fig. 5 reflect the large latitude band chosen for analysis. As discussed in Hudson et al. (2006), while the regimes do separate total ozone columns into distinct groups, there does remain a latitude dependence in total ozone within each regime. This latitude dependence in the ozone column is influenced by the latitude dependence in tropopause height; tropopause height decreases with increasing latitude. For example, high-latitude tropical profiles will generally have lower mean ozonepause heights than low-latitude tropical profiles, and could be similar to the mean ozonepause heights of midlatitude profiles. Therefore the large and overlapping distributions in Fig. 5 are a result of changes in sampling from year to year. The climatological zonal average ozonepause for 25°-60° N is also shown in Fig. 5 as a black line to illustrate the large deviations from the zonal mean seen when utilizing the method of meteorological regimes.

Figure 6a–d shows the column amounts for each regime for the altitude intervals 10–20 km, 20–30 km, 30–40 km, and 40–50 km, respectively. It should be noted that the column amount shown in Fig. 6a is only the stratospheric component. The line and color scheme are the same as in Fig. 5. The seasonal cycles of each regime in the lower stratosphere, seen in Fig. 6a, show recognizable features of the distribution of total ozone, e.g. the increase with latitude, and the spring maximum. As would be expected in this altitude region, the regimes show seasonal cycles with distinct amplitudes. Figure 6b shows the results for the 20–30 km region. This region is a transition

ACPD
8, 13375–13411, 2008

between the dynamically controlled lower stratosphere, and the photochemically controlled upper stratosphere (Logan, 1999; Staehelin et al., 2001); therefore the regimes show no clear distinction from one another. Figure 6c and 6d are in the upper stratosphere and as such, show summer maximums in column amount (Logan, 1999). As expected, no distinction between regimes is seen in Fig. 6c and 6d.

Figure 7a–d shows the HALOE climatologies seen in Fig. 4 (solid lines) in addition to climatologies calculated using data from SAGE (dash dot dash lines). The color scheme is the same as in Fig. 4. The one sigma standard deviations for the SAGE climatologies were on the order or smaller than those for HALOE, so they were not included on the figure. As anticipated, similar to the HALOE climatologies, distinct ozonepause heights and lower profile shapes in the lower stratosphere are seen in the SAGE climatologies. The climatologies agree very well in the lower stratosphere for every regime, and every month. The tropical mean profiles in month of September show the worst agreement between the two instruments; however, their 1□ distributions would overlap. While both SAGE and HALOE are solar occultation instruments which provide measurements over a broad range of latitudes, there are differences in the sampling patterns. In fact, the number of coincident measurements between the two instruments is small (Morris et al., 2002). Another difference between the two instruments is the wavelength region where ozone absorption is measured. HALOE measures ozone in the infrared region of the spectrum (9.6 μm), whereas SAGE measures in the visible (0.6 μm). These differences make the agreement seen in Fig. 7 all the more impressive, and emphasizes the decrease in atmospheric variability in the UTLS when within a meteorological regime.

While in the lower stratosphere the SAGE and HALOE climatologies agree very well, the agreement between the two climatologies appears to deteriorate above approximately 25 km. This difference in the mid to upper stratosphere (around 33 km) is a reflection of the difference in sampling between the two instruments as discussed above. Figure 7b in particular is an example of this. At around 33 km, the SAGE tropical and midlatitude climatologies are similar, whereas the HALOE tropical and midlatitude cli-

ACPD
8, 13375–13411, 2008

matologies differ by over 1 ppmv. This is due to the fact that the HALOE sampling in June shows a bimodal distribution in latitude, with the majority of measurements taken that month occurring at the lowest and highest latitudes analyzed. Because those measurements at lower latitudes are more likely to be classified into the tropical regime, while those at higher latitudes are more likely to be classified into the mid-latitude or polar regimes, the climatologies show distinct values in the mid to upper stratosphere. The SAGE sampling clusters around a smaller range of latitudes, and therefore the mid to upper stratosphere values are similar, regardless of regime. If the profiles from 25°–60° N were classified into latitude bands, and not meteorological regimes, they would be more clearly distinct in the mid and upper stratosphere. Figure 8 shows three climatological profiles for March. The red represents the low-latitude profiles (25°–33° N), the green represents mid-latitude profiles (38°–46° N), and the blue represents high-latitude profiles (51°–60° N). The dashed lines are the one-sigma standard deviation. The chemistry-dominated region above ~25 km shows three different ozone peak mixing ratio altitudes and values. The lower stratosphere shows three different tropopause heights, reflecting the decrease in tropopause height with latitude. However, in contrast to the March climatologies shown in Fig. 4, the distributions overlap significantly. This again emphasizes the dominance of the synoptic field on the distribution of ozone in the lower stratosphere, and therefore, the total column amount.

5 Water vapor profile classification

Both ozone and water vapor mixing ratios increase with altitude in the lower and mid stratosphere, but whereas ozone mixing ratios in the troposphere are smaller than in the stratosphere, the troposphere is much wetter than the stratosphere. Hence, in segregating profiles by meteorological regime we might expect to find variations which differ from those observed in ozone. Because of the very large water vapor mixing ratios in the troposphere relative to the stratosphere, the seasonal variations in water vapor mixing ratios in the lowermost stratosphere are particularly sensitive to

ACPD
8, 13375–13411, 2008

stratosphere-troposphere exchange (Pan et al., 2000). Dessler and Sherwood (2004) estimate that convection increases extratropical water vapor at 380 K by 40%, while decreasing ozone by only a few percent. Water vapor in this region of the atmosphere has a long chemical lifetime, and is considered to be an excellent tracer of motion and transport in the lower stratosphere (Brasseur and Solomon 1984; Rosenlof 2002; Chiou et al., 2006). Water vapor in the extratropical lower stratosphere will be a combination of high mixing ratio air that has subsided from the upper stratosphere, low mixing ratio air that has traveled across the cold tropical tropopause, and very high mixing ratio air that has crossed from the troposphere to the stratosphere outside the tropics. The extent to which an air parcel is influenced by these sources of water vapor should be sensitive to which meteorological regime it is in.

5.1 One day

The total ozone field, boundaries, and location of each HALOE sunset measurement taken on 18 February 1998 can be seen in Fig. 1. Similar to Fig. 2, Fig. 9 shows all of the water vapor measurements made on this day. Each profile in Fig. 9 that has been classified into a regime is in color, and the key indicates the profile's number and longitude. All of the profiles show a minimum below 20 km, and then increasing mixing ratios with increasing altitude, corresponding to the formation of water vapor through the oxidation of methane (Letexier et al., 1988). The variability around the hygropause, which we take here to be simply the altitude of the lowest water vapor mixing ratio, is much larger than the variability seen around the ozonepause region in Fig. 2. Figure 10a–c show the individual profiles that have been classified into the polar, midlatitude, and tropical regimes, respectively. Profiles 10 and 14, seen in Fig. 10a have similar hygropause heights, around 12–13 km. Profile 2 has a hygropause height at ~14.5 km; however another local minimum exists below, at around 11 km. Also worth noting is the increased variability in the value of the minimum. In Fig. 10a, the hygropause values range from ~3–4 ppmv. Figure 10b shows the five profiles classified as midlatitude. These profiles have hygropause heights ranging from 13–15 km. The

ACPD
8, 13375–13411, 2008

two tropical profiles are shown in Fig. 10c, and have hygropause heights at 14.5 and 15.2 km.

Thus, water vapor profiles show distinct differences between meteorological regimes, but unlike ozone where the difference is well described by differences in ozonepause altitude, the distinction in water vapor is sometimes more clearly seen not by the altitude but by the mixing ratio at the hygropause. Thus, the low water vapor mixing ratios in the two tropical profiles in Fig. 10c suggest that most of this air has recently passed through the tropical tropopause and therefore not experienced significant methane oxidation. These low water vapor values, and examinations of the profiles in Fig. 3c, support the interpretation that the tongue of low ozone seen in Fig. 1 is tropical in nature and not the result of mixing in of ozone depleted air from the arctic vortex.

5.2 Climatology

Monthly water vapor climatologies were calculated using data from both SAGE and HALOE for the period 1997–2004 between 25° and 60° N. Figure 11a–d shows the March, June, September, and December monthly water vapor climatologies, respectively, calculated using data from HALOE. The one-sigma standard deviations are shown as dashed lines, and the numbers of profiles used in the climatologies are shown in the right-hand subpanels. The subtropical, midlatitude, and polar regimes are shown as red, green, and blue lines, respectively.

The March and December climatologies show that the types of differences between meteorological regimes observed in the 18 February 1998 profiles are observed over several months. The tropical regime profiles have the driest and highest hygropause, suggesting that air at the hygropause in this regime has recently passed through the tropical tropopause. During this time of year, there is a strong transport barrier between the tropics and mid-latitudes in the lowermost stratosphere [Prados et al., 2003], helping to maintain the distinction between the hygropause mixing ratios in the tropical and midlatitude regimes. While the December climatology does not show any clear distinction between the midlatitude and polar profiles, the March and June climatolo-

ACPD

8, 13375–13411, 2008

gies do show a hygropause which does, just as in the case of the ozonepause for those months, decrease in altitude from the tropical to midlatitude regime and from the midlatitude to the polar regime. In September, the tropical and midlatitude climatologies come close to overlapping, for reasons discussed in Sect. 4.2.

Similar to Fig. 5, Fig. 12 shows the monthly mean hygropause heights for the tropical (red), midlatitude (green) and polar (blue) regimes. The one-sigma standard deviations of the means are shown as dashed lines, and the zonal mean between 25° and 60° N is shown as a black solid line. All three regimes show similar seasonal cycles, all having a summer maximum and winter minimum. The midlatitude and polar climatologies in this figure show that the mean hygropause is higher in altitude than the ozonepause between 25° and 60° N. This is also true in the tropical regime from April to December. While the ozonepause provides a good indication of a local vertical chemical mixing barrier, the possible transport of high water vapor mixing ratios into the lowermost stratosphere without crossing the cold tropical tropopause can result in a hygropause which is well above the tropopause. Such transport is especially prevalent in the summer (Dessler and Sherwood 2004) and helps to accentuate the seasonal variation observed in the hygropause levels shown in Fig. 12 relative to variation seen in the ozonepause levels shown in Fig. 5.

The same climatological HALOE profiles, along with climatologies calculated using data from SAGE are seen in Fig. 13a–d. On these figures, the solid lines represent the HALOE data, the dash-dot-dash lines represent the SAGE data, and the color scheme is the same as the previous four figures. Overall, the SAGE climatologies show good agreement with those of HALOE. The water vapor climatologies do not agree with each other as well as the ozone climatologies, but the profile variations as a function of regime for each month generally do agree. Thus, while the hygropause in the SAGE measurements is at a slightly higher altitude than that from the HALOE measurements, the difference between the regimes is consistent. For both SAGE and HALOE the mean altitude of the hygropause increases from the polar, to the midlatitude and finally to the tropical regime in all four months shown in Fig. 13. In addition, in March, where the

ACPD
8, 13375–13411, 2008

altitude distinction is most clearly seen, the water vapor mixing ratios measured by both instruments at the hygropause decrease in the same sequence.

6 Summary and conclusions

Ozone and water vapor profiles from HALOE and SAGE were classified into meteorological regimes as defined by Hudson et al. (2003, 2006). This was done on both daily and seven-year climatological timescales to determine over what altitude ranges and seasons the profiles of both constituents showed distinct characteristics within each regime.

When HALOE data were analyzed for a single day, 18 February 1998, each regime exhibited a distinct range of ozonepause heights, with the tropical regime containing the highest, and the polar regime the lowest. Similar results were found for water vapor, although the difference in the altitudes of the hygropause, from one regime to the next, was less than for ozone. In fact, at times the primary distinction between regimes for the water vapor profiles was not the altitude of the hygropause, but the mixing ratio at the hygropause. In addition, high variability in the mixing ratio at the hygropause was observed. For example, within the tropical regime alone, the hygropause values differed by ~1 ppmv. The HALOE measurements on this day were taken over ~4° latitude, but cover a wide range of longitudes. Within this narrow latitude band, each regime showed distinct characteristics in the UTLS. Based on our calculated ozonepause heights, a zonal average over this latitude band at any altitude from 8–16km would contain both tropospheric and stratospheric air.

Monthly profile climatologies were calculated for each regime using ozone and water vapor data from SAGE and HALOE from 1997–2004 for 25°–60° N. The ozone climatologies showed distinct ozonepause heights and profile shapes in the UTLS within each regime. The 1□ distributions of these climatologies showed little to no overlap. The month of September showed the least distinction between regimes. This is mostly due to the weak latitudinal gradient in the total ozone field. There was excellent agree-

ACPD
8, 13375–13411, 2008

ment between the HALOE and SAGE climatologies in the UTLS despite differences in the latitude sampling of the measurements, chosen wavelengths, and retrieval techniques.

The distinction between meteorological regimes deteriorates above ~25 km. This corresponds well with previous estimates of the extent, in altitude, of meteorological influence on stratospheric ozone profiles. (Koch et al., 2002; Newchurch et al., 2003). While the SAGE and HALOE ozone climatologies agree well in the UTLS, at altitudes above 25 km the effect of differences in the latitudinal sampling of the two instruments becomes apparent. To examine this further, stratospheric column ozone amounts at various altitude intervals were examined. From 10–20 km, each regime was characterized by distinctly different column amounts. This distinction diminished, and then disappeared as higher altitudes were analyzed. Additionally, when the March profiles for 1997–2004 from 25°–60° N were classified into low, middle, and high latitude bands, a clear distinction between latitude bands in the mid to upper stratosphere was obtained, whereas the distributions in the UTLS were not as clearly distinct as when the profiles were separated by meteorological regime.

The larger variability within a regime seen in the one-day classification of water vapor profiles was also seen in the monthly climatologies. The variability for each regime increases below ~15 km for both instruments, corresponding to a known increase in instrument uncertainty and increased atmospheric variability (Thomason et al., 2004). Despite these large uncertainties, the same general features are seen in the two sets of climatologies. For example, the tropical regime has the highest mean hygropause height, followed by the midlatitude, and then the polar. March shows the most distinction between regimes, displaying distinct hygropause heights, and mixing ratios for each regime. Similar to the ozone climatologies, September showed the weakest differentiation.

We have shown here that, below ~25 km, each regime is characterized by a unique ozone and water vapor profile shape. This distinction is greatest in the winter and spring and weaker in the summer and fall. By first classifying profiles into meteoro-

ACPD

8, 13375–13411, 2008

logical regimes, the lower stratosphere and upper troposphere can be isolated, which is essential for quantification of both chemical and transport processes in these regions. Hudson et al. (2003 and 2006) showed that each regime is also characterized by unique total ozone values, and that changes in the relative weighting of these regimes over time could contribute to trends in total ozone. These changes will also affect profile trends in the UTLS. Thus, similar to trends in total ozone, changes in the UTLS will be the result of both changes within each regime and changes in the contributions made by each regime over time.

Acknowledgements. The early part of this work was funded by a grant from the NASA Science Mission Directorate and later by the Naval Research Laboratory. This work was also performed in part while M. Follette held a National Research Council Research Associateship award at the Naval Research Laboratory. The SAGE II data were processed and provided by the NASA Langley Research Center (NASA-LaRC) and the NASA Langley Radiation and Aerosols Branch; the HALOE data were obtained from the HALOE website: http://haloedata.larc.nasa.gov/home/index.php and the TOMS data were obtained from the TOMS website: http://toms.gsfc.nasa.gov/.

References

Bethan, S., Vaughan, G., and Reid, S. J.: A comparison of ozone and thermal tropopause heights and the impact of tropopause definition on quantifying the ozone content of the atmosphere, Q. J. Roy. Meteor. Soc., 122, 929–944, 1996.

Bhatt, P. P., Remsberg, E. E., Gordley, L. L., McInerney, J. M., Brackett, V. G., and Russell III, J. M.: An evaluation of the quality of Halogen Occultation Experiment ozone profiles in the lower stratosphere, J. Geophys. Res., 104, 9261–9275, 1999.

Bluestein, H. B.: Synoptic-dynamic meteorology in midlatitudes, Vol II, Oxford University Press, 594 pp., New York City, New York, USA, 1993.

Brasseur, G. and Solomon, S.: Aeronomy of the middle atmosphere, D. Reidel Publishing Company, Dordrecht, The Netherlands, 441 pp., 1984.

Brühl, C. and Co–authors: Halogen Occulation Experiment ozone channel validation, J. Geophys. Res., 101, 10 217–10 240, 1996.

Chiou, E. W., Thomason, L. W., and Chu, W. P.: Variability of stratospheric water vapor inferred from SAGE II, HALOE, and Boulder (Colorado) balloon measurements, J. Climate, 19, 4121–4133, 2006.
Chu, W. P., McCormick, M. P., Lenoble, J., Brogniez, C., and Pruvost, P.: SAGE II inversion algorithm, J. Geophys. Res., 94, 8339–8351, 1989.
Chu, W. P., Chiou, E. W., Larsen, J. C., Thomason, L. W., Rind, D., Buglia, J. J., Oltmans, S., McCormick, M. P., and McMaster, L. M.: Algorithms and sensitivity analyses for Stratospheric Aerosol and Gas Experiment II water vapor retrieval, J. Geophys. Res., 98, 4857–4866, 1993.
Cunnold, D. M., Chu, W. P., Barnes, R. A., McCormick, M. P., and Veiga, R. E.: Validation of SAGE II ozone measurements, J. Geophys. Res., 94, 8447–8460, 1989.
Danielsen, E. F.: Stratospheric-tropospheric exchange based on radioactivity, ozone and potential vorticity, J. Atmos. Sci., 25, 502–518, 1968.
Defant, F. and Taba, H.: The threefold structure of the atmosphere and the characteristics of the tropopause, Tellus, 9, 259–274, 1957.
Dessler, A. E. and Sherwood, S. C.: Effect of convection on the summertime extratropical lower stratosphere, J. Geophys. Res., 109, D23301, doi:10.1029/2004JD005209, 2004.
Dobson, G. M., Harrison, D. N., and Lawrence, J.: Measurements of the amount of ozone in the Earth's atmosphere and its relation to other geophysical conditions – Part III, Proc. Roy. Soc. Lond., A122, 456–486, 1929.
Grooß, J.-U. and Russell, J. M.: Technical note: A stratospheric climatology for O_3, H_2O, CH_4, NO_x, HCl and HF derived from HALOE measurements, Atmos. Chem. Phys., 5, 2797–2807, 2005, http://www.atmos-chem-phys.net/5/2797/2005/.
Harries, J. E. and Co–authors: Validation of measurements of water vapor from the Halogen Occultation Experiment (HALOE), J. Geophys. Res., 101, 10 205-10 216, 1996.
Hervig, M. and McHugh, M.: Cirrus detection using HALOE measurements, Geophys. Res. Lett., 26, 719–722, 1999.
Hoinka, K. P., Claude, H., and Köhler, U.: On the correlation between tropopause pressure and ozone above central Europe, Geophys. Res. Lett., 23, 1753–1756, 1996.
Holton, J. R., Haynes, P. H., McIntyre, M. E., Douglass, A. R., Rood, R. B., and Pfister, L.: Stratosphere-troposphere exchange, Rev. Geophys., 33, 403–440, 1995.
Hudson, R. D., Frolov, A. D., Andrade, M. F., and Follette, M. B.: The total ozone field separated

into meteorological regimes, Part I: Defining the regimes, J. Atmos. Sci., 60, 1669–1677, 2003.
Hudson, R. D., Andrade, M. F., Follette, M. B., and Frolov, A. D.: The total ozone field separated into meteorological regimes, Part II: Northern Hemisphere midlatitude total ozone trends, Atmos. Chem. Phys., 6, 5183–5191, 2006, http://www.atmos-chem-phys.net/6/5183/2006/.
Kalnay, E. and Co–authors: The NCEP/NCAR 40-Year reanalysis project, B. Am. Meteorol. Soc., 77, 437–471, 1996.
Karol, I. L., Klyagina, L. P., Frolov, A. D., and Shalamyansky, A. M.: Fields of ozone and temperature within the boundaries of air masses, Meteor. Gidrol., 10, 47–52, 1987.
Kistler, R. and Co–authors: The NCEP–NCAR 50–Year reanalysis: Monthly means CD-ROM and documentation, B. Am. Meteorol. Soc., 82, 247–267, 2001.
Kley, D., Stone, E. J., Henderson, W. R., Drummond, J. W., Harrop, W. J., Schmeltekopf, A. L., Thompson, T. L., and Winkler, R. H.: In situ measurements of the mixing ratio of water vapor in the stratosphere, J. Atmos. Sci., 36, 2513–2524, 1979.
Kley, D. and Co–authors: SPARC assessment of upper tropospheric and stratospheric water vapor, WCRP 113, WMO/TD-1043, SPARC Rep. 2, World Clim. Res. Program, Geneva, Switzerland, 312 pp., 2000.
Koch, G., Wernli, H., Staehelin, J., and Peter, T.: A lagrangian analysis of stratospheric ozone variability and long-term trends above Payerne (Switzerland) during 1970–2001, J. Geophys. Res., 107 (D19), 4373, doi:10.1029/2001JD001550, 2002.
Letexier, H., Solomon, S., and Garcia, R. R.: The role of molecular hydrogen and methane oxidation in the water vapor budget of the stratosphere, Q. J. Roy. Meteor. Soc., 114, 281–295, 1988.
Logan, J. A.: An analysis of ozonesonde data for the lower stratosphere: Recommendations for testing models, J. Geophys. Res., 104, 16 151-16 170, 1999.
Morris, G. A., Gleason, J. F., Russell, J. M., Schoeberl, M. R., and McCormick, M. P.: A comparison pf HALOE v19 with SAGE II v 6.0 ozone observations using trajectory mapping, J. Geophys. Res., 107, 4177, doi:10.1029/2001JD000847, 2002.
Newchurch, M. J., Ayoub, M. A., Oltmans, S., Johnson, B., and Schmidlin, F. J.: Vertical distribution of ozone at four sites in the United States, J. Geophys. Res., 108(D1), 4031, doi:10.1029/2002JD002059, 2003.
Pan, L. L., Hintsa, E. J., Stone, E. M., Weinstock, E., and Randel, W. J.: Seasonal cycle

of water vapor and saturation mixing ratio in the extratropical lowermost stratosphere, J. Geophys. Res., 105, 26 519–26 530, 2000.
Pan, L. L., Randel, W. J., Gary, B. L., Mahoney, M. J., and Hintsa, E. J.: Definitions and sharpness of the extratropical tropopause: A trace gas perspective, J. Geophys. Res., 109, D23103, doi:10.1029/2004JD004982, 2004.
Petzoldt, K., Naujokat, B., and Neugebohren, K.: Correlation between stratospheric temperature, total ozone, and tropospheric weather systems, Geophys. Res. Lett., 21, 1203–1206, 1994.
Prados, A. I., G. E., Nedoluha, R. M., Bevilaqua, D. R., Allen, K. W., Hoppel, and Marenco, A.: POAM III ozone in the upper troposphere and lowermost stratosphere: Seasonal variability and comparisons to aircraft observations, J. Geophys. Res., 108(D7), 4218, doi:10.1029/2002JD002819, 2003.
Randall, C. E. and Co–authors: Validation of POAM III ozone: Comparisons with ozonesondes and satellite data, J. Geophys. Res., 108, 4367, doi:10.1029/2002JD002944, 2003.
Randel, W. J., Seidel, D. J., and Pan, L. L.: Observational characteristics of double tropopauses, J. Geophys. Res., 112, D07309, doi:10.1029/2006JD007904, 2007.
Reed, R.: A study of a characteristic type of upper-level frontogenesis, J. Meteorol., 12, 226–237, 1955.
Rosenlof, K. H.: Transport changes inferred from HALOE water and methane measurements, J. Meteorol. Soc. Japan, 80, 831–848, 2002.
Russell, J. M. and Co–authors: The halogen occultation experiment, J. Geophys. Res., 98, 10 777–10 797, 1993.
Schubert, S. D. and Munteanu, M. J.: An analysis of tropopause pressure and total ozone correlations, Mon. Weather Rev., 116, 569–582, 1988.
Shalamyanskiy, A. M. and Romashkina, A. K.: Distribution and variation in the total ozone concentration in various air masses, Izv. Acad. Sci. USSR, Atmos. Ocean. Phys., 16, 931–937, 1980.
Shapiro, M. A.: Further evidence of the mesoscale and turbulent structure of upper level jet stream-frontal zone systems, Mon. Weather Rev., 106, 1100–1111, 1978.
Shapiro, M. A.: Turbulent mixing within tropopause folds as a mechanism for the exchange of chemical constituents between the stratosphere and troposphere, J. Atmos. Sci., 37, 994–1004, 1980.
Shapiro, M. A., Krueger, A. J., and Kennedy, P. J.: Nowcasting the position and intensity of jet

streams using a satellite-borne Total Ozone Mapping Spectrometer, Nowcasting, Academic Press, San Diego, California, USA, 137–145, 1982.
Shapiro, M. A.: Dropwinsonde observations of an Icelandic low and a Greenland mountain-lee wave, Mon. Weather Rev., 113, 680–683, 1985.
Staehelin, J., Harris, N. R. P., Appenzeller, C., and Eberhard, J.: Ozone trends: A review, Rev. Geophys., 39, 231–290, 2001.
Steinbrecht, W., Claude, H., Köhler, U., and Hoinka, K. P.: Correlations between tropopause height and total ozone: Implications for long-term changes, J. Geophys. Res., 103, 19 183–19 192, 1998.
Taha, G., Thomason, L. W., Burton, S. P.: Comparison of Stratospheric Aerosol and Gas Experiment (SAGE) II Version 6.2 water vapor with balloon-borne and spacebased measurements, J. Geophy. Res., 109, D18313, doi:10.1029/2004JD004859, 2004.
Thomason, L. W., Burton, S. P., Iyer, N., Zawodny, J. M., and Anderson, J. M.: A revised water vapor product for the Stratospheric Aerosol and Gas Experiment (SAGE) II Version 6.2 data set, J. Geophy. Res., 109, D06312, doi:10.1029/2003JD004465, 2004.
Varotsos, C., Cartalis, C., Vlamakis, A., Tzanis, C., Keramitsoglou, I.: The long-term coupling between column ozone and tropopause properties, J. Clim., 17, 3843–3854, 2004.
Wang, H. J., Cunnold, D. M., Thomason, L. W., Zawodny, J. M., and Bodeker, G. E.: Assessment of SAGE Version 6.1 ozone data quality, J. Geophy. Res., 107, 4691, doi:10.1029/2002JD002418, 2002.
Wellemeyer, C. G., Bhartia, P. K., McPeters, R. D., Taylor, S. L., and Ahn, C.: A new release of data from the Total Ozone Mapping Spectrometer (TOMS), SPARC Newsletter, 22, 37–38, available at: www.aero.jussieu.fr/~sparc, 2004.
WMO: SPARC/IOC/GAW Assessment of trends in the vertical distribution of ozone:1998 Ozone Research and Monitoring Project, Rep., 43, 289 pp., 1998.
WMO: Scientific assessment of ozone depletion: 2002 Global Research and Monitoring Project, Rep. 47, Geneva, Switzerland, 498 pp., 2003.

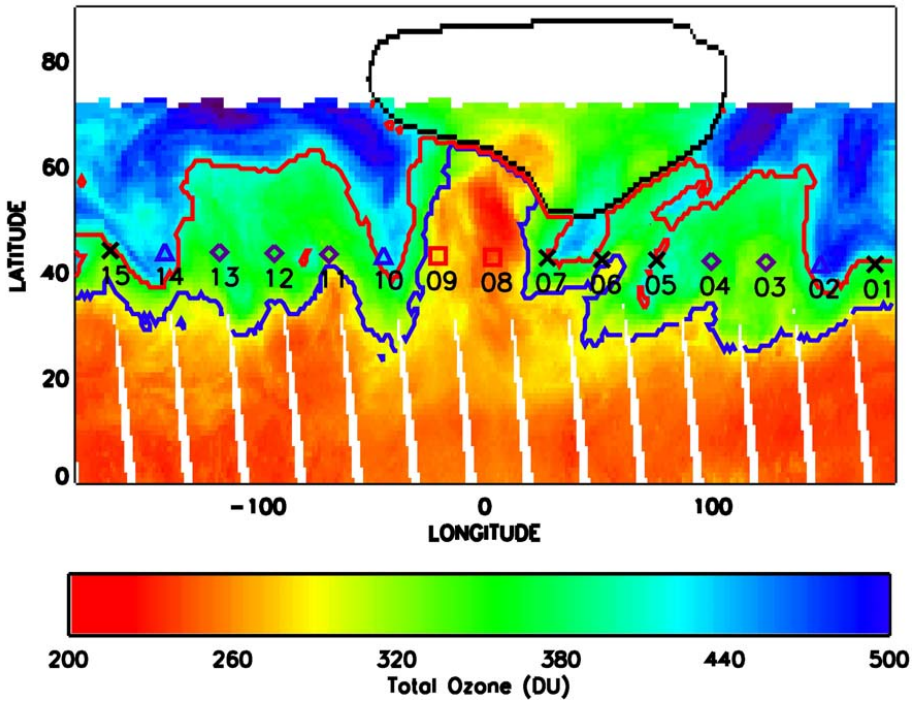

Fig. 1. EP TOMS total ozone field for 18 February 1998. The subtropical, polar, and arctic boundaries are shown as blue, red, and black lines, respectively. Each symbol represents a HALOE sunset measurement for this day, and has been numbered 01 through 15. The color and choice of each symbol corresponds to its classification: red squares – tropical, purple diamonds – midlatitude, blue triangles – polar, and black Xs – boundary.

ACPD

8, 13375–13411, 2008

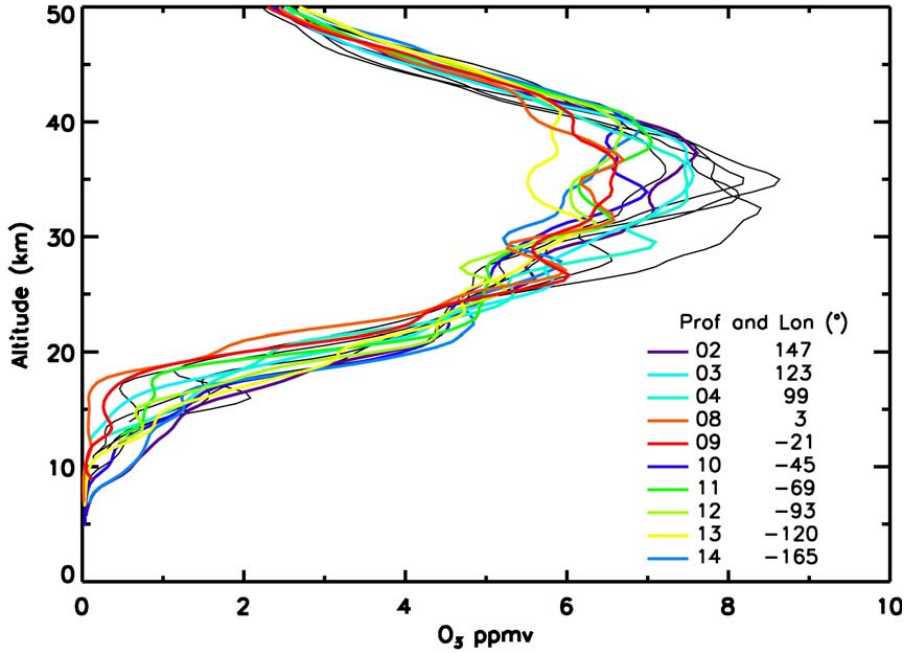

Fig. 2. HALOE ozone profiles that correspond to the symbols on Fig. 1 for 18 February 1998. Profiles that were classified into a meteorological regime are shown in color and listed on the figure. Profiles that fell within a pixel of the boundary are shown in black.

ACPD
8, 13375–13411, 2008

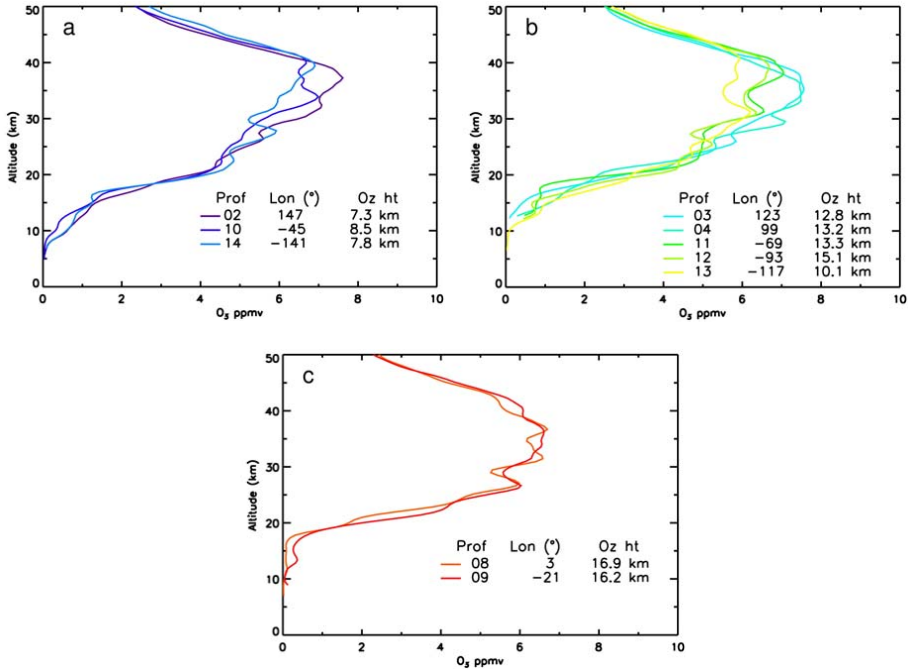

Fig. 3. HALOE ozone profiles that correspond to the colored symbols on Fig. 1 for 18 February 1998 for the **(a)** polar regime, **(b)** midlatitude regime, and **(c)** tropical regime. The profile numbers, longitudes, and ozonepause heights are also listed.

ACPD
8, 13375–13411, 2008

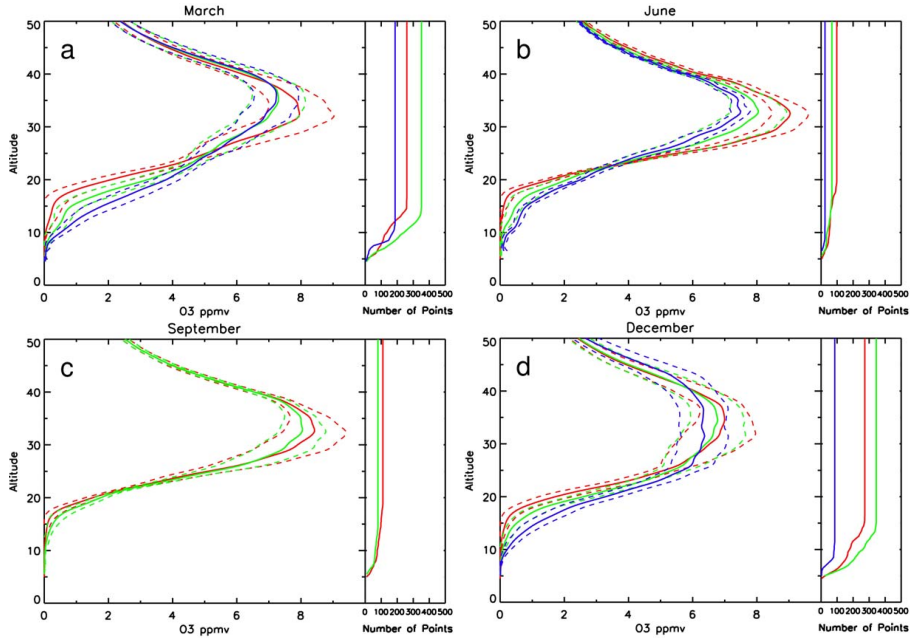

Fig. 4. HALOE ozone profile climatologies calculated from 1997–2004 between 25° and 60° N for **(a)** March, **(b)** June, **(c)** September, and **(d)** December. The one-sigma standard deviations of the mean are shown as dashed lines, and the number of points is shown on the right. The color scheme is: red – tropical, green – midlatitude, and blue – polar.

ACPD

8, 13375–13411, 2008

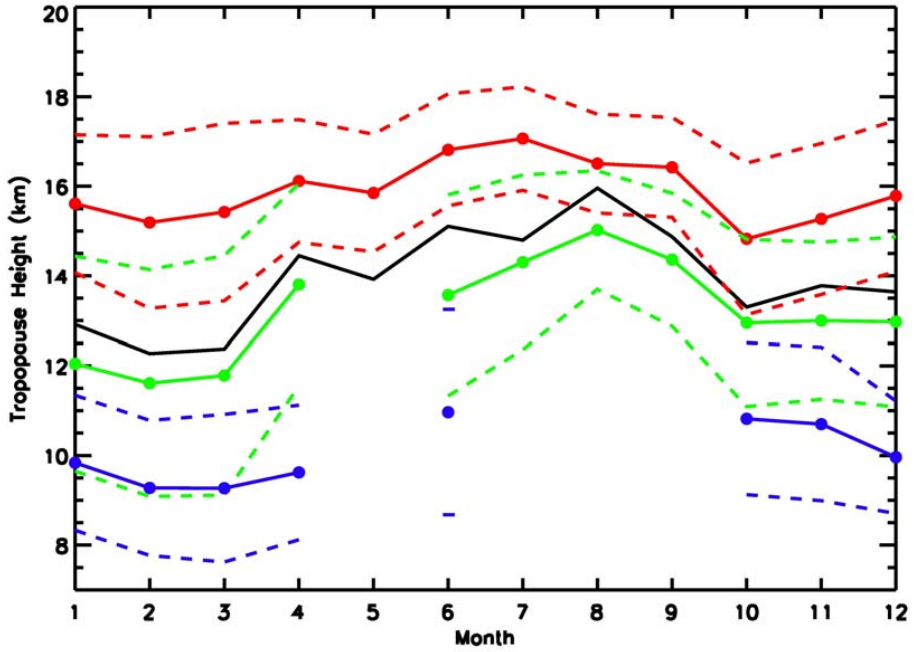

Fig. 5. Ozonepause height climatologies calculated from 1997–2004 between 25° and 60° N for the tropical (red), midlatitude (green), and polar (blue) regimes. The black line is the zonally averaged ozonepause height. The one-sigma standard deviations of the means are shown as dashed lines and are shown in the same color scheme as the means.

ACPD

8, 13375–13411, 2008

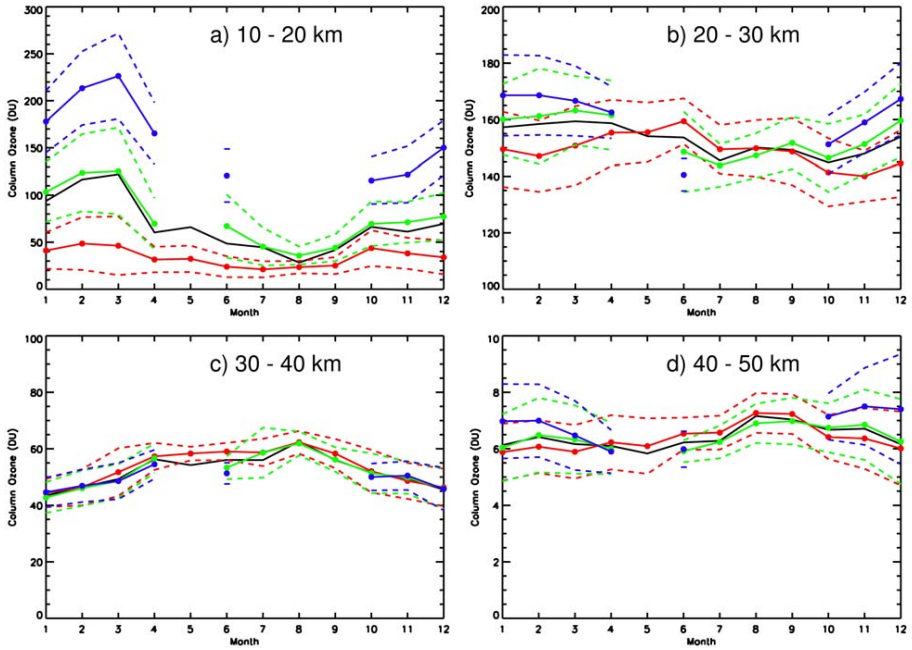

Fig. 6. Stratospheric column ozone climatologies (in DU) calculated from 1997–2004 between 25° and 60° N for **(a)** 10–20 km, **(b)** 20–30 km, **(c)** 30–40 km, and **(d)** 40–50 km. Note the different scales. The solid lines with filled circles indicate the tropical (red), midlatitude (green), and polar (blue) regimes. The black line is the zonally averaged stratospheric column ozone. The onesigma standard deviations of the means are shown as dashed lines and are shown in the same color scheme as the means.

ACPD
8, 13375–13411, 2008

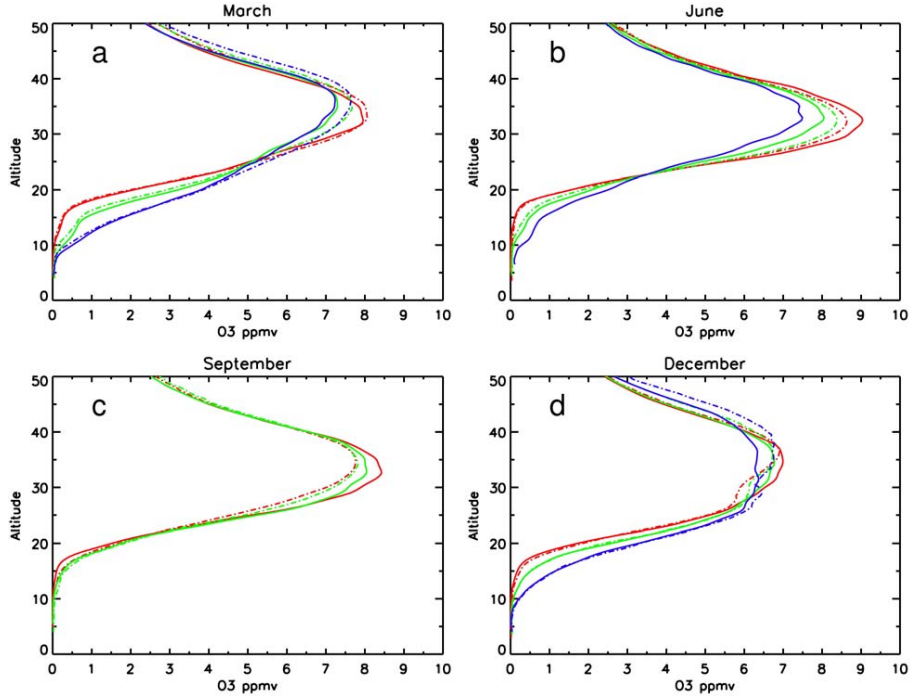

Fig. 7. HALOE (solid lines) and SAGE (dash dot dash lines) ozone profile climatologies calculated from 1997–2004 between 25° and 60° N for **(a)** March, **(b)** June, **(c)** September, and **(d)** December. The color scheme is: red – tropical, green – midlatitude, and blue – polar.

ACPD

8, 13375–13411, 2008

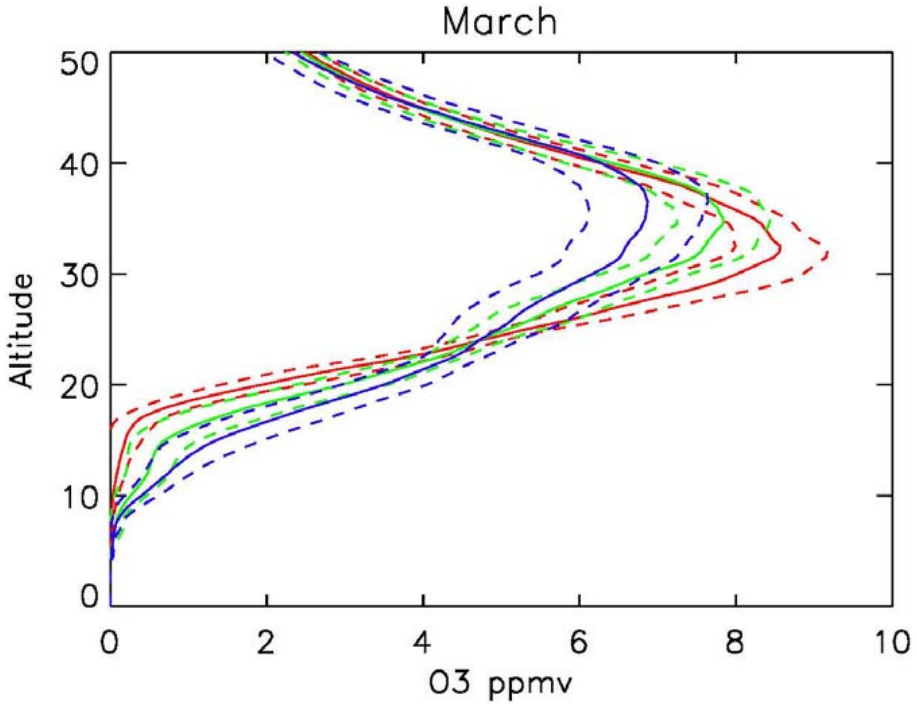

Fig. 8. HALOE ozone profile climatologies calculated from 1997–2004 between 25° and 60° N for March. The red indicates the low latitude (25°–33° N) climatology, the green indicates the middle latitude (38°–46°N) climatology, and the blue indicates the high latitude (51°–60° N) climatology. The dashed lines are the one-sigma standard deviation.

ACPD
8, 13375–13411, 2008

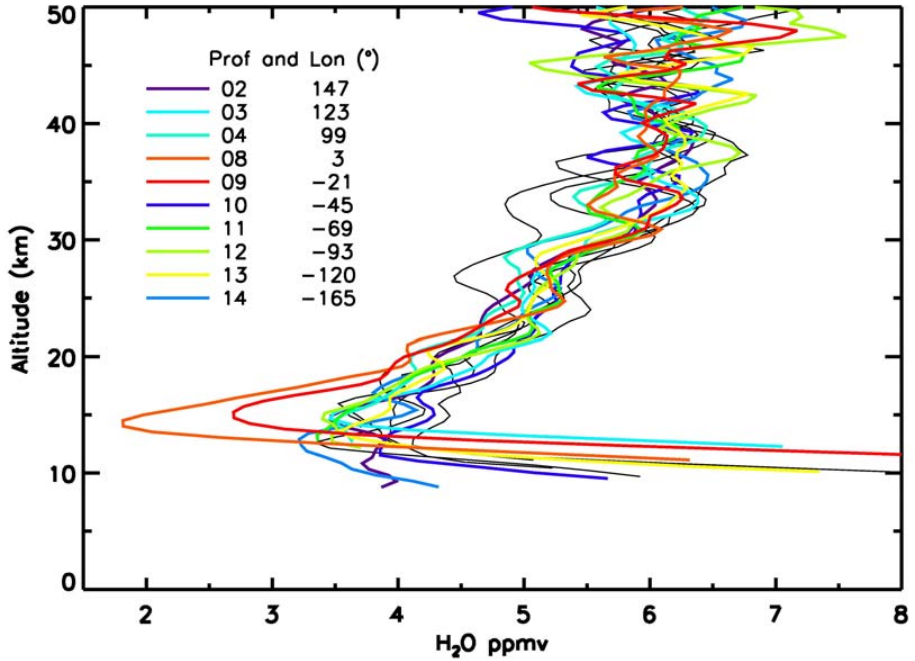

Fig. 9. HALOE water vapor profiles that correspond to the symbols on Fig. 1 for 18 February 1998. Profiles that were classified into a meteorological regime are shown in color and listed on the figure. Profiles that fell within a pixel of the boundary are shown in black.

ACPD
8, 13375–13411, 2008

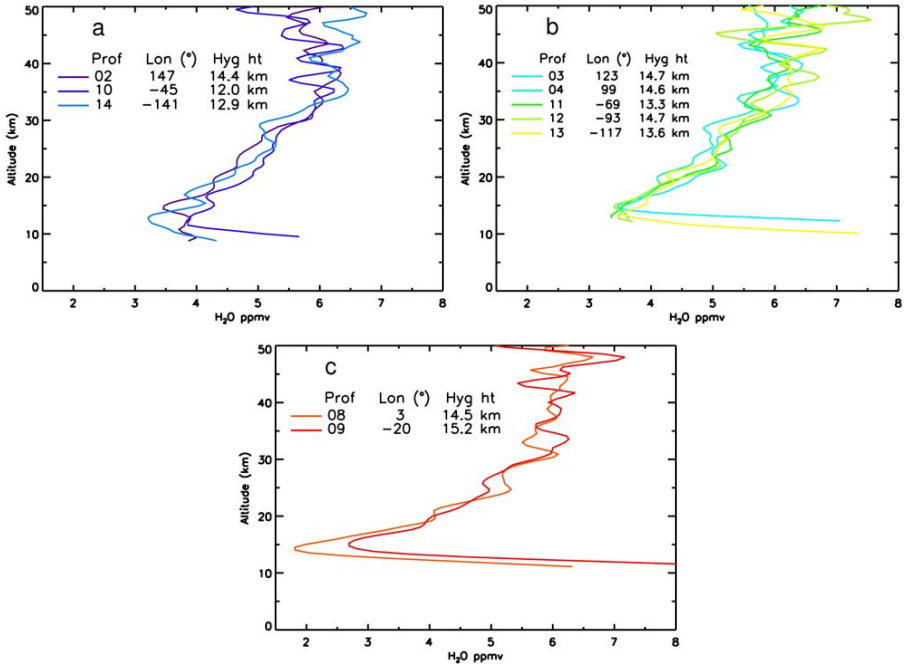

Fig. 10. HALOE water vapor profiles that correspond to the colored symbols on Fig. 1 for 18 February 1998 for the **(a)** polar regime, **(b)** midlatitude regime, and **(c)** tropical regime. The profile numbers, longitudes, and hygropause heights are also listed.

ACPD
8, 13375–13411, 2008

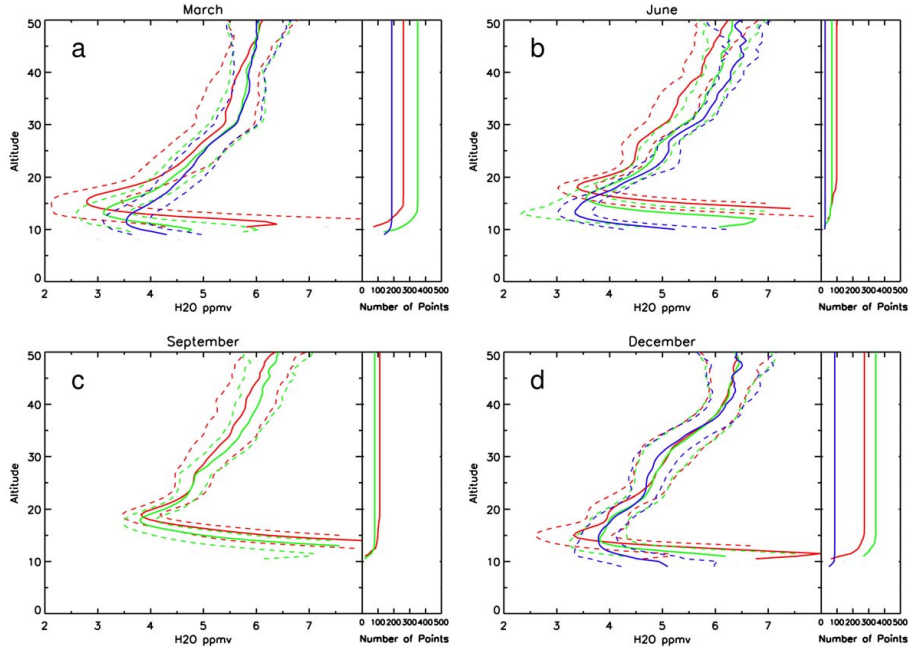

Fig. 11. HALOE water vapor profile climatologies calculated from 1997–2004 between 25° and 60° N for **(a)** March, **(b)** June, **(c)** September, and **(d)** December. The one-sigma standard deviations are shown as dashed lines, and the number of points are shown on the right. The color scheme is: red – tropical, green – midlatitude, and blue – polar.

ACPD

8, 13375–13411, 2008

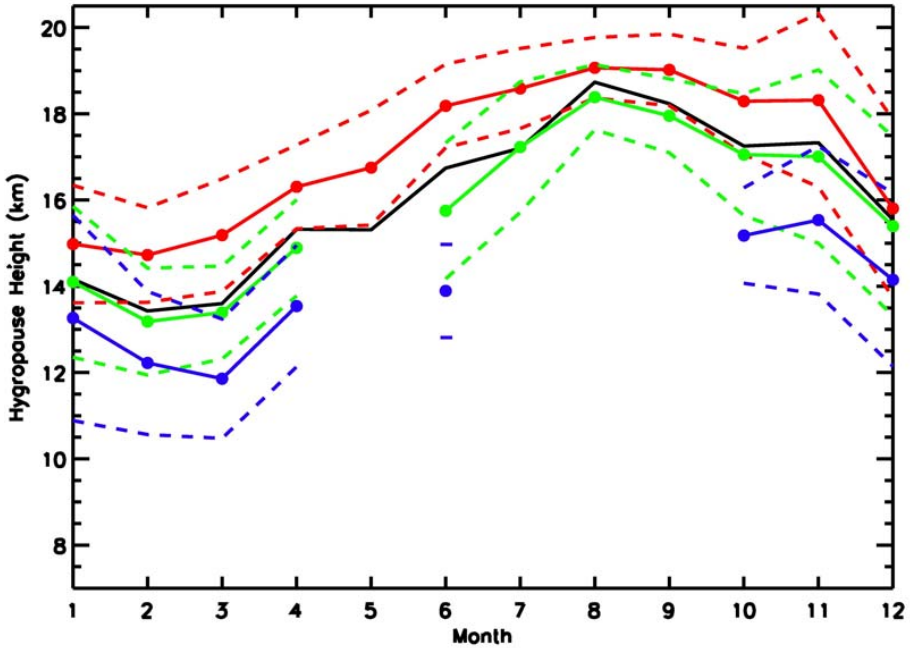

Fig. 12. Hygropause height climatologies calculated from 1997–2004 between 25° and 60° N for the tropical (red), midlatitude (green), and polar (blue) regimes. The black line is the zonally averaged hygropause height. The one-sigma standard deviations of the means are shown as dashed lines and are shown in the same color scheme as the means.

ACPD
8, 13375–13411, 2008

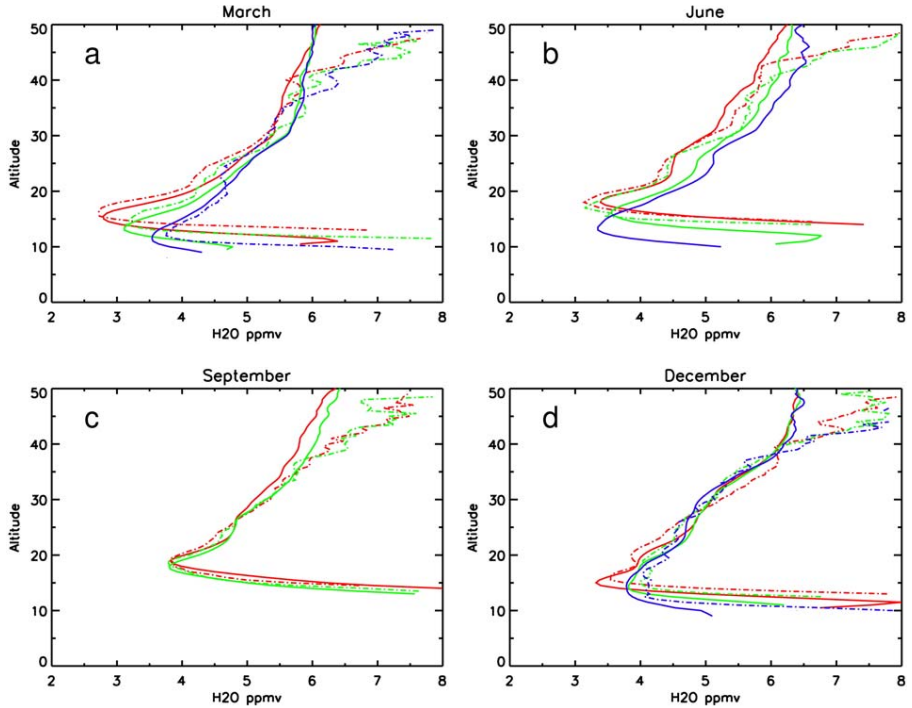

Fig. 13. HALOE and SAGE water vapor profile climatologies calculated from 1997–2004 between 25° and 60° N for **(a)** March, **(b)** June, **(c)** September, and **(d)** December. HALOE data is shown as solid lines, and SAGE data is shown as dash-dot-dash lines. The color scheme is: red – tropical, green – midlatitude, and blue – polar.

ACPD

8, 13375–13411, 2008